Chinese Journal of Electronics
vol. 33, no. 1, pp. 231–244, January 2024
https://doi.org/10.23919/cje.2022.00.384

RESEARCH ARTICLE

Drug-Target Interactions Prediction Based on Signed Heterogeneous Graph Neural Networks

Ming CHEN[1], Yajian JIANG[1], Xiujuan LEI[2], Yi PAN[3], Chunyan JI[4], and Wei JIANG[1]

1. *College of Information Science and Engineering, Hunan Normal University, Changsha 410081, China*
2. *School of Computer Science, Shaanxi Normal University, Xi'an 710119, China*
3. *Faculty of Computer Science and Control Engineering, Shenzhen Institute of Advanced Technology, Chinese Academy of Sciences, Shenzhen 518055, China*
4. *Computer Science Department, BNU-HKBU United International College, Zhuhai 519087, China*

Corresponding author: Yi PAN, Email: yi.pan@siat.ac.cn
Manuscript Received November 10, 2022; Accepted March 21, 2023

Abstract — Drug-target interactions (DTIs) prediction plays an important role in the process of drug discovery. Most computational methods treat it as a binary prediction problem, determining whether there are connections between drugs and targets while ignoring relational types information. Considering the positive or negative effects of DTIs will facilitate the study on comprehensive mechanisms of multiple drugs on a common target, in this work, we model DTIs on signed heterogeneous networks, through categorizing interaction patterns of DTIs and additionally extracting interactions within drug pairs and target protein pairs. We propose signed heterogeneous graph neural networks (SHGNNs), further put forward an end-to-end framework for signed DTIs prediction, called SHGNN-DTI, which not only adapts to signed bipartite networks, but also could naturally incorporate auxiliary information from drug-drug interactions (DDIs) and protein-protein interactions (PPIs). For the framework, we solve the message passing and aggregation problem on signed DTI networks, and consider different training modes on the whole networks consisting of DTIs, DDIs and PPIs. Experiments are conducted on two datasets extracted from DrugBank and related databases, under different settings of initial inputs, embedding dimensions and training modes. The prediction results show excellent performance in terms of metric indicators, and the feasibility is further verified by the case study with two drugs on breast cancer.
Keywords — Drug-target interactions, Signed heterogeneous network, Link sign prediction, Graph neural networks.
Citation — Ming CHEN, Yajian JIANG, Xiujuan LEI, *et al.*, "Drug-Target Interactions Prediction Based on Signed Heterogeneous Graph Neural Networks," *Chinese Journal of Electronics*, vol. 33, no. 1, pp. 231–244, 2024. doi: 10.23919/cje.2022.00.384.

I. Introduction

The prediction of drug-target interactions (DTIs) is of great significance to the fields of drug design and drug development. However, traditional biological experiments are time-consuming and cost-effective, so it has prompted more people to pay their attention to the use of computers to assist in predicting DTIs [1]–[6].

At present, there are many machine learning methods for DTIs prediction. Traditional approaches, including network/graph embedding models, matrix factorization or feature-based methods, either focus on extracting associations between drugs and proteins or depend on information from node attributes. Compared with traditional methods, as a deep learning branch for irregular data, graph neural networks (GNNs) have shown excellent performance in mining biomedical networks [7]–[11]. GNNs can make better use of both node characteristics and network structures [7], and their powerful computing platforms [12] provide convenient model training. Currently, GNNs have been the popular methods in DTIs prediction [13], [14].

Most of the existing DTIs prediction methods ignore the specific interaction patterns between drugs and targets, however, enriching a drug-target network with information of functional nature like the sign of the in-

Associate Editor: Prof. Hongkai XIONG, Shanghai Jiao Tong University.

teractions allows to explore a series of network properties of key importance in the context of computational drug combinatorics [15], [16]. For example, by attaching signs to the mechanisms of action, we are able to quantify the amount of synergism (i.e., when coherence prevails over incoherence) in a drug pair, and to classify all drug pairs accordingly.

In this study, we construct signed networks of drugs and targets according to pharmacological DTIs. Additionally, we extract information from interactions between drugs and their associated target proteins. But, how to deal with DTIs prediction on signed heterogeneous networks is still an open issue. To solve the problem, we dedicate signed heterogeneous graph neural networks (SHGNNs), further put forward a method for signed DTIs prediction, called SHGNN-DTI.

1. Related work

There are a large amount of DTIs prediction studies. Their methods are roughly divided into two categories: traditional approaches and deep learning methods. In terms of the prediction form, existing studies either explore whether the drug can interact with the target or exploit more informative details of DTIs.

Many machine learning directions have been applied to DTIs prediction and most of them either focus on node features or links between nodes. The former calculates node representation vectors of drugs and targets respectively and then trains a discriminator to predict DTIs. Typical node embedding methods include graph/network based embedding [17] etc. And classifiers such as support vector machine [18] and random forest [19], can act as a discriminator. However, traditional node representation based approaches need two-stage training process and cannot fully extract deep and complex associations between drugs and targets. Another direction is link-based ways including matrix factorization (MF) [20] and random walk (RW) [21]. MF uses the product of two or more low-rank matrices to approximate the association matrix, while RW [21] is widely used in methods based on graph theories. But, they commonly ignore explicit and natural integration of node features and graph structures. Other directions, such as hybrid methods [22] and ensemble learning, also have potentials in DTIs prediction. However, the lack of computing platform support hampers the development of traditional methods on large-scale data.

Recently, GNNs, as a branch of deep learning dedicated for irregular data, show excellent performance in graph mining research [7]–[11], [23]. Compared with traditional models, GNNs not only make better use of node characteristics and network structures [7], but also inherit end-to-end learning frameworks from deep learning; In addition, there are powerful computing platforms developed [12]. Until now, many kinds of GNNs have been explored to tackle with the heterogeneous graphs [9], [24]. Spectral convolution based GNNs [25], attention based GNNs [13], meta-path based GNNs [14] have shown their applications on DTIs networks.

However, most current studies take DTIs prediction as a binary classification problem [1], [22] which lays a good foundation for the initial stage of drug development. In order to further accelerate the process of drug discovery, it is far from enough to explore whether the drug can interact with the target [17]. To overcome the disadvantages of binary classification, some researchers turn to exploit more detailed information of DTIs. When browsing DrugBank [26], we find more than 35 mechanisms of action modes of DTIs and most of them can be reasonably classified as positive or negative on targets. It is reported that signed DTIs facilitate the study of the comprehensive mechanism of drug combinatorics [15], [16], [27], which is the main motivation of this paper.

There are some signed GNNs extended from unsigned and raw models, but it is still open whether they are applicable to signed DTIs networks. One extension is from spectral GNNs, which explores frequency analysis with signed graph Laplacians [28], [29] and commonly adapts to homogeneous graphs. Another direction is to combine spatial GNNs with a notable social theory on signed graphs such as balance theory.

Typical models include signed graph convolutional network (SGCN) [30] and signed bipartite graph neural network (SBGNN) [31]. To our best knowledge, existing signed GNNs focus on either signed graphs with the same entities [30] or simple bipartite graphs [31] separately. Hence, they are unable to handle the complexities brought by both drug-drug interactions (DDIs) and protein-protein interactions (PPIs) information. In addition, it is still open whether the most commonly used balance theory is applicable to signed DTIs networks. Actually, unsatisfactory results are observed in our initial attempt to directly apply some of these models on signed DTIs bipartite networks.

2. Our contributions

In this study, we first model DTIs on signed heterogeneous networks, and then put forward a signed GNN framework for DTIs prediction by designing information propagation process and considering different training settings. Our contributions are concluded as follows.

- In terms of interaction modes between drugs and targets, we model DTIs prediction on signed heterogeneous networks. DTIs are categorized and expressed as signed links [15], [16], [27], according to pharmacological drug-target interactions in DrugBank [26] database, and hence form a signed bipartite network. In addition, we construct a two-layer signed heterogeneous network, by extracting DDIs, drug chemical features from PubChem [32], and PPIs from String [33].
- We propose SHGNN-DTI, to realize the end-to-end DTIs sign prediction, which takes drug-target embedding pair as the input and jointly train a DTIs discriminator. To deal with message passing and aggrega-

tion on signed DTIs networks, we dedicate signed aggregation on bipartite graphs. Furthermore, we propose a three-module framework to handle two additional unsigned graphs, and train it with considerations of either cooperative or independent mode and whether sharing weights. It is noted that our SHGNN-DTI not only adapts to signed bipartite networks, but also could naturally incorporate auxiliary information from DDIs and PPIs.

• Comprehensive experiments on two DTIs networks are conducted to verify the validity of our prediction model. In terms of several performance metrics, its performance greatly exceeds the baselines. The effect of initial features of nodes, training modes and embedding dimensions are also discussed. Ablation study further illustrates the role of three modules. In addition, we provide the case study on two drugs for breast cancer, and find that seven new DTIs out of their Top-10 links have support from other literature, which verifies the feasibility of SHGNNs-based DTIs prediction.

II. Problem Descriptions

In this section, we model DTIs on signed heterogeneous networks. Firstly, the DTIs is modeled on a signed bipartite network, and then extended onto a two-level signed heterogeneous network.

When browsing DrugBank [26], we see many possible mechanisms of drug-target actions. For example, a drug activates or inhibits a target acting as an agonist or antagonist, as a potentiator or blocker, as an inducer or suppressor, and so on. There are different types of targets such as proteins, macro molecules, nucleic acids, and small molecules, etc. Drug-target actions can be roughly divided into positive or negative relations [15] and naturally represented as signed links. As shown in Table 1, the action modes of drugs and targets are represented as signed links [15]. Activator, agonist and other positive types are classified into positive effects and represented by the label $+1$, whereas types with negative effects like inhibitor and antagonist are labeled with -1. For example, Pilocarpine is an activator of Muscarinic acetylcholine receptor, and the link is represented by $+1$. The drug Bivalirudin, as an inhibitor of Prothrombin, inhibits thrombin action by binding the catalytic site of thrombin to the external site of anion binding, and the link is indicated by -1.

Table 1 Drug modes of action and edge signs

Edge sign	Action modes in DrugBank
Positive (+)	Agonist; partial agonist; activator; stimulator; inducer; positive allosteric modulator; potentiator; positive modulator
Negative (−)	Inhibitor; inhibitory allosteric modulator; inhibitor competitive; antagonist; partial antagonist; negative modulator; inverse agonist; blocker; suppressor; desensitize the target; neutralizer; reducer
Not classifiable (0)	Otherwise

It is noted that some modes are labeled with 0, e.g., "modulators", "binder", "cleavage", because they are impossible to classify with a sign, and hence cannot be included in our analysis. In this case, we do not construct an edge between the drug and the target.

In this study, we further extract information from interactions between drugs and their associated target proteins, to model a two-level signed heterogeneous network. For all the drugs, we also crawl their features and interaction information from DrugBank [26]. Meanwhile, we search the known human protein interaction data in String [33] database to obtain the interaction information among targets. For DDIs and PPIs, we use 1 to indicate the known interaction and 0 for the others.

Figure 1 shows the DTIs prediction on signed networks. The problem is to determine the sign of drug-target action, i.e., $? \in \{+, -\}$. Given a set of drugs $D = (D_1, D_2, \ldots, D_n)$, a set of targets $T = (T_1, T_2, \ldots, T_m)$ and their signed edges $E_{\mathrm{DT}} = \{e_{ij}, i = 1, 2, \ldots, n, j = 1, , 2, \ldots, m\}$, we predict new DTIs on a signed bipartite network $G_{\mathrm{DT}} = (D, T, E_{\mathrm{DT}})$ (shown in Figure 1(a)) according to Table 1. Additionally, with the help of unsigned DDIs network $G_D = (D, \boldsymbol{A}_D, E_D)$ and PPIs network $G_T = (T, \boldsymbol{A}_T, E_T)$, the problem becomes DTIs prediction on the two-level signed heterogeneous network as shown in Figure 1(b).

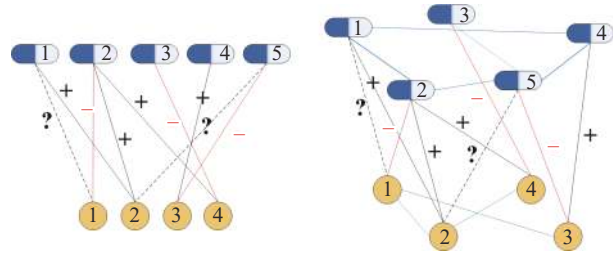

(a) A signed bipartite network (b) A two-level signed heterogeneous network

Figure 1 DTIs prediction on signed networks. The problem is to determine the link sign between a drug and a target for (a) a signed bipartite network and (b) a two-level signed heterogeneous network.

III. SHGNNs-Based DTIs Prediction Methods

The positive and negative edges represent two polarization relations between drugs and targets, but coexistence of negativity and heterogeneity brings challenges to the extension of the existing GNNs. As we know, current popular GNNs-based approaches mainly work on unsigned graphs, which will aggregate the neighbor information in the same way for both positive and negative edges. Even though some signed GNNs have been developed, the graph was assumed to have the same kind of entities or be simple bipartite graphs, and thus, they are not directly applicable to handle the complexities that are brought by drug pairs and target pairs.

In this section, we propose SHGNNs for DTIs prediction on drug-target networks. SHGNN-DTI works following the framework described in Figure 2. Firstly, it employs SHGNN to obtain embedding results of drugs and targets. Secondly, a drug-target pair, i.e., $(\boldsymbol{z}_{D_i}, \boldsymbol{z}_{T_j})$, which is concatenated from above embeddings, is taken as an input of a DTIs discriminator to predict the DTI sign. Our SHGNNs and the DTIs discriminator are jointly trained with the loss function described in the last sub-section. It is noted that, the framework still works on signed bipartite networks via ignoring Module2 and Module3 directly.

To enhance the readability and understandability, Table 2 provides key symbols used in SHGNN-DTI.

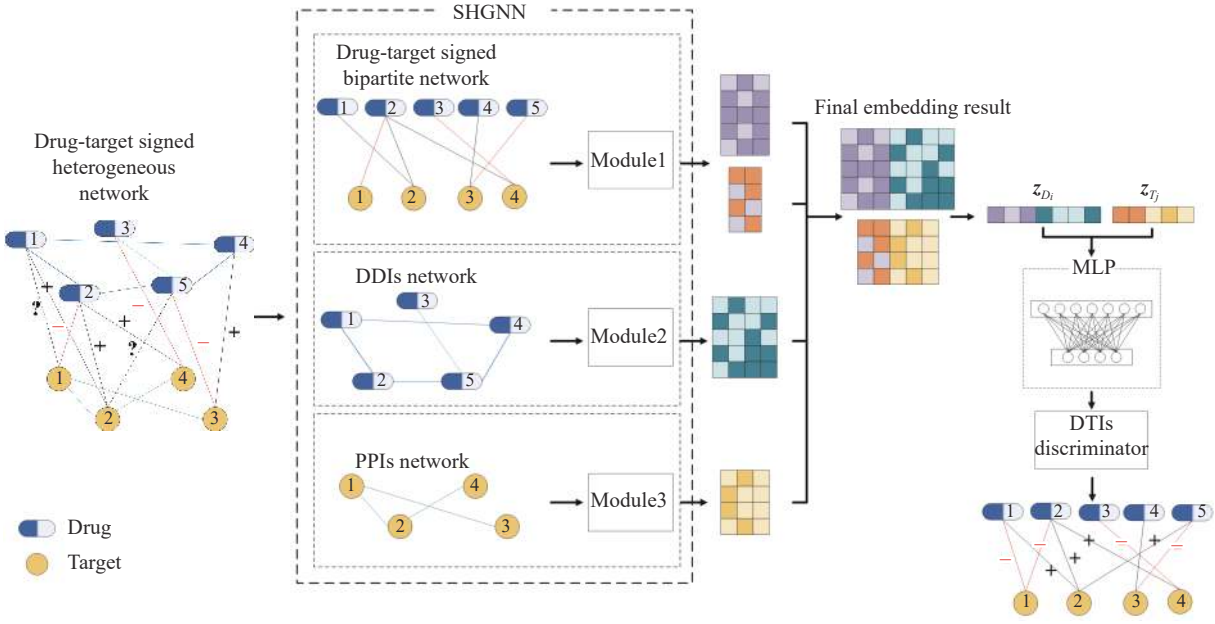

Figure 2 DTIs prediction based on SHGNNs. It employs a SHGNN model to obtain embedding results of drugs and targets, and then discriminates the sign of concatenated embeddings of a drug-target pair. The SHGNN and the discriminator are jointly trained with a loss function. When SHGNN works on only the DTIs subnetwork, Module2 and Module3 are missed.

Table 2 Key symbols in SHGNNs

Symbols	Descriptions
$\boldsymbol{h}_{D_i}^{(0)}, \boldsymbol{h}_{T_j}^{(0)}$	Initial features of drug D_i and target T_j
$\boldsymbol{h}_{D_i}^{\mathrm{DTI}(l)}$, $\boldsymbol{h}_{T_j}^{\mathrm{DTI}(l)}$	Inputs of Module1 in l-th layer
$\boldsymbol{h}_{D_i}^{\mathrm{DDI}(l)}$, $\boldsymbol{h}_{T_j}^{\mathrm{PPI}(l)}$	Inputs of Module2 and Module3 in l-th layer
$\boldsymbol{z}_{D_i}$, $\boldsymbol{z}_{T_j}$	Final embedding of D_i and T_j
$\boldsymbol{h}_{D_i}^{P(l)}, \boldsymbol{h}_{D_i}^{N(l)}, \boldsymbol{h}_{D_i}^{D(l)}$	Hidden representations of D_i in l-th layer
$\boldsymbol{h}_{T_j}^{P(l)}, \boldsymbol{h}_{T_j}^{N(l)}, \boldsymbol{h}_{T_j}^{T(l)}$	Hidden representations of T_j in l-th layer
$\boldsymbol{\Theta}_D^{P(l)}, \boldsymbol{\Theta}_D^{N(l)}$	Learnable parameter matrices of drugs in l-th layer on the DTIs subnetwork
$\boldsymbol{\Theta}_T^{P(l)}, \boldsymbol{\Theta}_T^{N(l)}$	Learnable parameter matrices of targets in l-th layer on the DTIs subnetwork
$\boldsymbol{\Theta}_D^{D(l)}, \boldsymbol{\Theta}_T^{T(l)}$	Learnable parameter matrices in l-th layer on the DDIs and PPIs subnetworks
_C	The cooperative mode
_I	The independent mode
_S	The same kind of nodes share $\boldsymbol{\Theta}$ in different modules
CS	Chemical structures of drugs
AD	The link vectors of drugs
AP	The link vectors of targets

1. The proposed SHGNNs

In the design of signed GNNs, there are two key problems. The first one is how to propagate messages on DTIs networks and aggregate information for both drug and target nodes. As shown in Figure 3, the drug (target) has signed relations. Inspired by SGCN [30] that is customized on signed graphs with homogeneous entities, we solve the first problem and then propose SHGNN model to study node embedding results on signed bipartite network. The second problem is how to extend SHGNN to additionally integrate DDIs and PPIs, and solve the training problem. Here, we propose three-module SHGNNs and put forward an end-to-end learning framework that adapts to both signed bipartite networks and two-level heterogeneous networks.

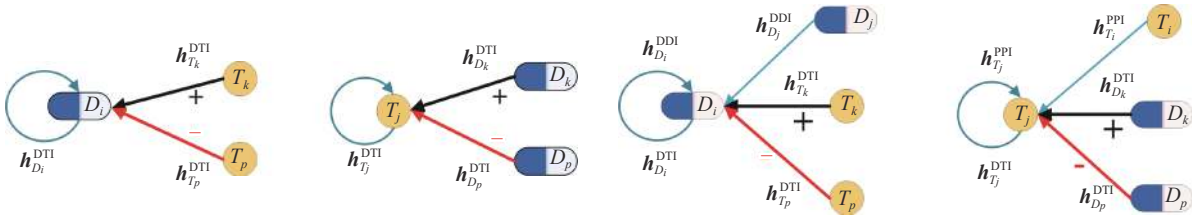

(a) Information propagation on signed bipartite network (b) Information propagation on signed heterogeneous network

Figure 3 Information propagation on DTIs networks. (a) Signed bipartite network; (b) Signed heterogeneous network.

1) SHGNN on signed bipartite networks

We dedicate message passing and aggregation process based on signed relations following the framework of the simple SGCN variant [30].

SGCN is the first GNN model dedicated on signed graphs. Its raw version, which is built on balanced theory and one-level homogeneous networks, is not directly applicable to our two-level DTIs signed networks. Here, we borrow the aggregation in its variant. The l-th SGCN layer is calculated in terms of signed relations [30] among the same kind of entities:

$$\boldsymbol{h}_i^{P(l)} \triangleq \sigma\left(\boldsymbol{\Theta}^{P(l)}\left[\sum_{k\in\mathcal{N}_i^+}\frac{\boldsymbol{h}_k^{(l-1)}}{|\mathcal{N}_i^+|}, \boldsymbol{h}_i^{(l-1)}\right]\right)$$

$$\boldsymbol{h}_i^{N(l)} \triangleq \sigma\left(\boldsymbol{\Theta}^{N(l)}\left[\sum_{k\in\mathcal{N}_i^-}\frac{\boldsymbol{h}_k^{(l-1)}}{|\mathcal{N}_i^-|}, \boldsymbol{h}_i^{(l-1)}\right]\right)$$

where $\boldsymbol{h}_i^{P(l)}$ and $\boldsymbol{h}_i^{N(l)}$ are hidden states of node i, following positive and negative links, respectively. $\mathcal{N}_i^+$ ($\mathcal{N}_i^-$) denotes the set of positive (negative) neighbors of v_i. $\boldsymbol{\Theta}^{P(l)}$ and $\boldsymbol{\Theta}^{N(l)}$ are learnable parameter matrices for linear transformation, and each $\boldsymbol{\Theta}$ matrix includes two parts corresponding to neighbors and the node itself, respectively. σ is an activation function which is set as tanh. The concatenation of hidden states is taken as the input for the next layer, i.e., $\boldsymbol{h}_i^{(l)} \triangleq \boldsymbol{h}_i^{P(l)} \parallel \boldsymbol{h}_i^{N(l)}$.

Inspired by SGCN [30], we first solve the message aggregation and node update problem on signed DTIs bipartite networks. Let $\boldsymbol{h}_k^{'}$ be the output of linear transformation on v_k. The underly message passing and aggregation in simple SGCN work as follows:

$$\boldsymbol{h}_i^P = \sum_{k\in\mathcal{N}_i^+}\frac{\boldsymbol{h}_k^{'}}{|\mathcal{N}_i^+|} + \boldsymbol{h}_i^{'}, \quad \boldsymbol{h}_i^N = \sum_{k\in\mathcal{N}_i^-}\frac{\boldsymbol{h}_k^{'}}{|\mathcal{N}_i^-|} + \boldsymbol{h}_i^{'}$$

They are responsible for positive and negative neighbors, respectively. For DTIs bipartite networks, Figure 3 (a) illustrates information propagation, where each node has heterogeneous neighbors. We denote the positively (negatively)-linked target neighbor set of D_i by $\mathcal{N}_{D_i}^+$ ($\mathcal{N}_{D_i}^-$). Analogously, we define $\mathcal{N}_{T_j}^+$, $\mathcal{N}_{T_j}^-$ for targets. After information propagation, nodes' contents are updated as follows:

$$\boldsymbol{h}_{D_i}^P = \sum_{T_k\in\mathcal{N}_{D_i}^+}\frac{\boldsymbol{h}_{T_k}^{'}}{|\mathcal{N}_{D_i}^+|} + \boldsymbol{h}_{D_i}^{'}, \quad \boldsymbol{h}_{D_i}^N = \sum_{T_k\in\mathcal{N}_{D_i}^-}\frac{\boldsymbol{h}_{T_k}^{'}}{|\mathcal{N}_{D_i}^-|} + \boldsymbol{h}_{D_i}^{'}$$

$$\boldsymbol{h}_{T_j}^P = \sum_{D_k\in\mathcal{N}_{T_j}^+}\frac{\boldsymbol{h}_{D_k}^{'}}{|\mathcal{N}_{T_j}^+|} + \boldsymbol{h}_{T_j}^{'}, \quad \boldsymbol{h}_{T_j}^N = \sum_{D_k\in\mathcal{N}_{T_j}^-}\frac{\boldsymbol{h}_{D_k}^{'}}{|\mathcal{N}_{T_j}^-|} + \boldsymbol{h}_{T_j}^{'}$$

Let $\boldsymbol{h}_{D_i}^{\mathrm{DTI}(l-1)}$ and $\boldsymbol{h}_{T_j}^{\mathrm{DTI}(l-1)}$ denote the inputs to the l-th layer. With the consideration of linear transformation and activation, the l-layer embedding process on signed bipartite networks is

$$\begin{cases}\boldsymbol{h}_{D_i}^{P(l)} \triangleq \sigma\left(\boldsymbol{\Theta}_D^{P(l)}\left[\sum_{T_k\in\mathcal{N}_{D_i}^+}\frac{\boldsymbol{h}_{T_k}^{\mathrm{DTI}(l-1)}}{|\mathcal{N}_{D_i}^+|}, \boldsymbol{h}_{D_i}^{\mathrm{DTI}(l-1)}\right]\right)\\ \boldsymbol{h}_{D_i}^{N(l)} \triangleq \sigma\left(\boldsymbol{\Theta}_D^{N(l)}\left[\sum_{T_k\in\mathcal{N}_{D_i}^-}\frac{\boldsymbol{h}_{T_k}^{\mathrm{DTI}(l-1)}}{|\mathcal{N}_{D_i}^-|}, \boldsymbol{h}_{D_i}^{\mathrm{DTI}(l-1)}\right]\right)\end{cases} \tag{1}$$

$$\begin{cases}\boldsymbol{h}_{T_j}^{P(l)} \triangleq \sigma\left(\boldsymbol{\Theta}_T^{P(l)}\left[\sum_{D_k\in\mathcal{N}_{T_j}^+}\frac{\boldsymbol{h}_{D_k}^{\mathrm{DTI}(l-1)}}{|\mathcal{N}_{T_j}^+|}, \boldsymbol{h}_{T_j}^{\mathrm{DTI}(l-1)}\right]\right)\\ \boldsymbol{h}_{T_j}^{N(l)} \triangleq \sigma\left(\boldsymbol{\Theta}_T^{N(l)}\left[\sum_{D_k\in\mathcal{N}_{T_j}^-}\frac{\boldsymbol{h}_{D_k}^{\mathrm{DTI}(l-1)}}{|\mathcal{N}_{T_j}^-|}, \boldsymbol{h}_{T_j}^{\mathrm{DTI}(l-1)}\right]\right)\end{cases} \tag{2}$$

Here, $l \in \{1, 2, \ldots, L\}$, $i \in \{1, 2, \ldots, n\}$, $j \in \{1, 2, \ldots, m\}$.

$\boldsymbol{\Theta}^{NN(l)} \triangleq \{\boldsymbol{\Theta}_D^{P(l)}, \boldsymbol{\Theta}_D^{N(l)}, \boldsymbol{\Theta}_T^{P(l)}, \boldsymbol{\Theta}_T^{N(l)}\}$ are learnable parameter matrices on the l-th layer.

We employ their concatenation as the input for the next layer, i.e.,

$$\boldsymbol{h}_{D_i}^{\mathrm{DTI}(l)} \triangleq \boldsymbol{h}_{D_i}^{P(l)} \parallel \boldsymbol{h}_{D_i}^{N(l)}, \boldsymbol{h}_{T_j}^{\mathrm{DTI}(l)} \triangleq \boldsymbol{h}_{T_j}^{P(l)} \parallel \boldsymbol{h}_{T_j}^{N(l)} \tag{3}$$

A L-layer SHGNN generate final embedding results by

$$\boldsymbol{z}_{D_i} \triangleq \boldsymbol{h}_{D_i}^{P(L)} \parallel \boldsymbol{h}_{D_i}^{N(L)}, \boldsymbol{z}_{T_j} \triangleq \boldsymbol{h}_{T_j}^{P(L)} \parallel \boldsymbol{h}_{T_j}^{N(L)}$$

Algorithm 1 outlines the process of SHGNNs on signed bipartite DTIs networks.

Algorithm 1 SHGNN on signed bipartite networks

Input: A signed bipartite network $G_{DT} = (D, T, E_{DT})$; $\boldsymbol{h}_{D_i}^{(0)} (i = 1, 2, \cdots, n)$, $\boldsymbol{h}_{T_j}^{(0)} (j = 1, 2, \cdots, m)$; the number of layers L.

Output: Low-dimension representations $\boldsymbol{z}_{D_i}$ and $\boldsymbol{z}_{T_j}$.

Initialization:

$\boldsymbol{h}_{D_i}^{\mathrm{DTI}(0)} \triangleq \boldsymbol{h}_{D_i}^{(0)}$, $i = 1, 2, \ldots, n$;

$\boldsymbol{h}_{T_j}^{\mathrm{DTI}(0)} \triangleq \boldsymbol{h}_{T_j}^{(0)}$, $j = 1, 2, \ldots, m$;

for $l \in \{1, 2, \ldots, L\}$ do

Calculate $\boldsymbol{h}_{D_i}^{P(l)}$ and $\boldsymbol{h}_{D_i}^{N(l)}$ using equation (1);

Calculate $\boldsymbol{h}_{T_j}^{P(l)}$ and $\boldsymbol{h}_{T_j}^{N(l)}$ using equation (2);

Update $\boldsymbol{h}_{D_i}^{\mathrm{DTI}(l)}$ and $\boldsymbol{h}_{T_j}^{\mathrm{DTI}(l)}$ by eqution (3);

Return $\boldsymbol{z}_{D_i} \triangleq \boldsymbol{h}_{D_i}^{\mathrm{DTI}(L)}$, $\boldsymbol{z}_{T_j} \triangleq \boldsymbol{h}_{T_j}^{\mathrm{DTI}(L)}$.

2) SHGNNs with additional DDIs and PPIs subnetworks

Since DDIs or PPIs represent very different semantics from heterogeneous DTIs, it needs to find out how to extend SHGNN defined on G_{DT} to cover G_D and G_T, and solve the training problem. Here, we divide all relations into three subnetworks, propagate the information in Figure 3(b) via applying the signed GNN layer to G_{DT} and introducing unsigned GNN layers for G_D and G_T. Then, we try several training modes for the three-module GNN framework.

As shown in Figure 2, SHGNNs obtain embedding results not only from the DTIs network via Module1 defined with above subsection, but also from the DDIs network and PPIs. For a drug node D_i, let $\boldsymbol{h}_{D_i}^{\mathrm{DDI}(l-1)}$ denotes the input to the l-layer of Module2 and $\mathcal{N}_{D_i}^{\mathrm{DDI}}$ denotes its neighbor nodes within the DDIs network. Similarly, we define $\boldsymbol{h}_{T_j}^{\mathrm{PPI}(l-1)}$ and $\mathcal{N}_{T_j}^{\mathrm{PPI}}$ for the target T_j on the PPIs network. Aggregation in Module2 and Module3 are

$$\boldsymbol{h}_{D_i}^{D(l)} \triangleq \sigma\left(\boldsymbol{\Theta}_D^{D(l)}\left[\sum_{D_k \in \mathcal{N}_{D_i}^{\mathrm{DDI}}} \frac{\boldsymbol{h}_{D_k}^{\mathrm{DDI}(l-1)}}{|\mathcal{N}_{D_i}^{\mathrm{DDI}}|}, \boldsymbol{h}_{D_i}^{\mathrm{DDI}(l-1)}\right]\right) \tag{4}$$

$$\boldsymbol{h}_{T_j}^{T(l)} \triangleq \sigma\left(\boldsymbol{\Theta}_T^{T(l)}\left[\sum_{T_k \in \mathcal{N}_{T_j}^{\mathrm{PPI}}} \frac{\boldsymbol{h}_{T_k}^{\mathrm{PPI}(l-1)}}{|\mathcal{N}_{T_j}^{\mathrm{PPI}}|}, \boldsymbol{h}_{T_j}^{\mathrm{PPI}(l-1)}\right]\right) \tag{5}$$

Here, $l \in \{1, 2, \ldots, L\}$, $i \in \{1, 2, \ldots, n\}$, $j \in \{1, 2, \ldots, m\}$. $\boldsymbol{\Theta}^{NN(l)} \triangleq \{\boldsymbol{\Theta}_D^{P(l)}, \boldsymbol{\Theta}_D^{N(l)}, \boldsymbol{\Theta}_D^{D(l)}, \boldsymbol{\Theta}_T^{P(l)}, \boldsymbol{\Theta}_T^{N(l)}, \boldsymbol{\Theta}_T^{T(l)}\}$ are learnable parameter matrices on the l-th layer.

After L layers, we concatenate results from all modules to get the final node representation:

$$\boldsymbol{z}_{D_i}^{\mathrm{DTI}} \triangleq \boldsymbol{h}_{D_i}^{P(L)} \parallel \boldsymbol{h}_{D_i}^{N(L)}, \boldsymbol{z}_{D_i}^{\mathrm{DDI}} \triangleq \boldsymbol{h}_{D_i}^{D(L)}, \boldsymbol{z}_{D_i} \triangleq \boldsymbol{z}_{D_i}^{\mathrm{DTI}} \parallel \boldsymbol{z}_{D_i}^{\mathrm{DDI}}$$
$$\boldsymbol{z}_{T_j}^{\mathrm{DTI}} \triangleq \boldsymbol{h}_{T_j}^{P(L)} \parallel \boldsymbol{h}_{T_j}^{N(L)}, \boldsymbol{z}_{T_j}^{\mathrm{PPI}} \triangleq \boldsymbol{h}_{T_j}^{T(L)}, \boldsymbol{z}_{T_j} \triangleq \boldsymbol{z}_{T_j}^{\mathrm{DTI}} \parallel \boldsymbol{z}_{T_j}^{\mathrm{PPI}}$$

The initial features of nodes, i.e., $\boldsymbol{h}_{D_i}^{\mathrm{DTI}(0)}, \boldsymbol{h}_{T_j}^{\mathrm{DTI}(0)}$, $\boldsymbol{h}_{D_i}^{\mathrm{DDI}(0)}, \boldsymbol{h}_{T_j}^{\mathrm{PPI}(0)}$, will be further discussed in our experiments later.

To train the three-module SHGNN, it needs to consider whether they interact with each other. One consideration is how to deal with outputs on the previous layer and feed them into the current layer. Another consideration is whether the same kind of nodes share learnable parameters in linear transformation. Here, we propose to train a SHGNN model in either cooperative or independent mode, and combine them with sharing weights.

i) The cooperative mode. In this case, three modules are trained cooperatively by setting the inputs with the same values for one kind of nodes:

$$\boldsymbol{h}_{D_i}^{\mathrm{DTI}(l)} = \boldsymbol{h}_{D_i}^{\mathrm{DDI}(l)} \leftarrow \boldsymbol{h}_{D_i}^{P(l)} \parallel \boldsymbol{h}_{D_i}^{N(l)} \parallel \boldsymbol{h}_{D_i}^{D(l)} \tag{6}$$

$$\boldsymbol{h}_{T_j}^{\mathrm{DTI}(l)} = \boldsymbol{h}_{T_j}^{\mathrm{PPI}(l)} \leftarrow \boldsymbol{h}_{T_j}^{P(l)} \parallel \boldsymbol{h}_{T_j}^{N(l)} \parallel \boldsymbol{h}_{T_j}^{T(l)} \tag{7}$$

As a result, in each layer Module 1 interacts with Module 2 and Module 3.

ii) The independent mode. In this case, three modules are trained independently within sub-networks. The input of each module is updated as its last embedding result as follows:

$$\boldsymbol{h}_{D_i}^{\mathrm{DTI}(l)} \leftarrow \boldsymbol{h}_{D_i}^{P(l)} \parallel \boldsymbol{h}_{D_i}^{N(l)}, \boldsymbol{h}_{D_i}^{\mathrm{DDI}(l)} \leftarrow \boldsymbol{h}_{D_i}^{D(l)} \tag{8}$$

$$\boldsymbol{h}_{T_j}^{\mathrm{DTI}(l)} \leftarrow \boldsymbol{h}_{T_j}^{P(l)} \parallel \boldsymbol{h}_{T_j}^{N(l)}, \boldsymbol{h}_{T_j}^{\mathrm{PPI}(l)} \leftarrow \boldsymbol{h}_{T_j}^{T(l)} \tag{9}$$

iii) Sharing weights. For both modes, we further consider whether the same kind of nodes share one parameter matrix, i.e. $\boldsymbol{\Theta}_{D_i}^{P(l)} = \boldsymbol{\Theta}_{D_i}^{N(l)} = \boldsymbol{\Theta}_{D_i}^{D(l)}$, $\boldsymbol{\Theta}_{T_j}^{P(l)} = \boldsymbol{\Theta}_{T_j}^{N(l)} = \boldsymbol{\Theta}_{T_j}^{T(l)}$. To keep the same embedding dimension, the independent mode replaces concatenation "$\parallel$" by addition "$+$" in equation (8)–(9), i.e.,

$$\boldsymbol{h}_{D_i}^{\mathrm{DTI}(l)} \leftarrow \boldsymbol{h}_{D_i}^{P(l)} + \boldsymbol{h}_{D_i}^{N(l)}, \boldsymbol{h}_{T_j}^{\mathrm{DTI}(l)} \leftarrow \boldsymbol{h}_{T_j}^{P(l)} + \boldsymbol{h}_{T_j}^{N(l)}$$

Algorithm 2 outlines the embedding generation on two-level DTIs networks. In Figure 4, we further show 2-

layer SHGNNs under either cooperative or independent mode.

Algorithm 2 SHGNNs on signed heterogeneous networks

Input: A signed bipartite network $G_{DT} = (D, T, E_{DT})$; a DDIs network $G_D = (D, \boldsymbol{A}_D, E_D)$; a PPIs network $G_T = (T, \boldsymbol{A}_T, E_T)$; $\boldsymbol{h}_{D_i}^{(0)}$ $(i = 1, 2, \ldots, n)$, $\boldsymbol{h}_{T_j}^{(0)}$ $(j = 1, 2, \ldots, m)$; the number of layers L.

Output: Low-dimension representations $\{\boldsymbol{z}_{D_i}$ and $\boldsymbol{z}_{T_j}.\}$

Initialization:

$\boldsymbol{h}_{D_i}^{\mathrm{DTI}(0)} = h_{D_i}^{\mathrm{DDI}(0)} \triangleq \boldsymbol{h}_{D_i}^{(0)}$, $i = 1, 2, \ldots, n$;

$\boldsymbol{h}_{T_j}^{\mathrm{DTI}(0)} = \boldsymbol{h}_{T_j}^{\mathrm{PPI}(0)} \triangleq \boldsymbol{h}_{T_j}^{(0)}$, $j = 1, 2, \ldots, m$;

for $l \in \{1, 2, \ldots, L\}$ do

Calculate $\boldsymbol{h}_{D_i}^{P(l)}$ and $\boldsymbol{h}_{D_i}^{N(l)}$ using equation (1);

Calculate $\boldsymbol{h}_{T_j}^{P(l)}$ and $\boldsymbol{h}_{T_j}^{N(l)}$ using equation (2);

Calculate $\boldsymbol{h}_{D_i}^{D(l)}$ using equation (4);

Calculate $\boldsymbol{h}_{T_j}^{T(l)}$ using equation (5);

Update $\boldsymbol{h}_{D_i}^{\mathrm{DTI}(l)}$ and $\boldsymbol{h}_{D_i}^{\mathrm{DDI}(l)}$ by equation (6) or equation (8);

Update $\boldsymbol{h}_{T_j}^{\mathrm{DTI}(l)}$ and $\boldsymbol{h}_{T_j}^{\mathrm{PPI}(l)}$ by equation (7) or equation (9);

Return $\boldsymbol{z}_{D_i} \triangleq \boldsymbol{h}_{D_i}^{\mathrm{DTI}(L)} \parallel \boldsymbol{h}_{D_i}^{\mathrm{DDI}(L)}, \boldsymbol{z}_{T_j} \triangleq \boldsymbol{h}_{T_j}^{\mathrm{DTI}(L)} \parallel \boldsymbol{h}_{T_j}^{PPI(L)}$.

2. The loss function

Taking the final drug-target pair $(\boldsymbol{z}_{D_i}, \boldsymbol{z}_{T_j})$ as an input, we employ a multilayer perception (MLP) to further extract characteristics of a drug-target pair, and then utilize a softmax regression classifier to discriminate the DTI type.

Here, we jointly train SHGNNs and the DTIs discriminator. Let $\boldsymbol{\Theta}^{NN} = \{\boldsymbol{\Theta}^{NN(1)}, \ldots, \boldsymbol{\Theta}^{NN(L)}\}$ include weight matrix parameters of L layers SHGNNs and the weight parameters $\boldsymbol{\Theta}^{MLP}$ for MLP, and $\boldsymbol{\Theta}^{R} = \{\boldsymbol{\Theta}_{+1}^{R}, \boldsymbol{\Theta}_{-1}^{R}\}$ denotes regression coefficients, where $\boldsymbol{\Theta}_{+1}^{R}$ $(\boldsymbol{\Theta}_{-1}^{R})$ is the positive (negative) edge type coefficient. The loss function is defined as follows:

$$\mathcal{L}(\boldsymbol{\Theta}^{NN}, \boldsymbol{\Theta}^{R}, \boldsymbol{\Theta}^{\mathrm{MLP}}) = \sum_{ij} -\omega_{e_{ij}} \sum_{c \in S} \mathbb{I}(e_{ij} = c) \log \frac{\exp(\boldsymbol{\Theta}_c^R \left[\mathrm{MLP}(\boldsymbol{z}_{D_i} || \boldsymbol{z}_{T_j})\right])}{\sum_{q \in S} \exp(\boldsymbol{\Theta}_q^R \left[\mathrm{MLP}(\boldsymbol{z}_{D_i} || \boldsymbol{z}_{T_j})\right]}$$

where $e_{ij} \in S$ represents the type of edge between drug D_i and target T_j, $S \in \{+1, -1\}$ and $\omega_{e_{ij}}$ denotes the weight associated with link type e_{ij}. $\mathbb{I}(\cdot)$ returns 1 if a given prediction is true, and 0 otherwise.

IV. Experimental Settings and Analyses

In this section, we conduct experiments on two datasets, one of which is newly extracted in this study from DrugBank [26] and related databases. First, our SHGNN shows excellent performance on signed bipartite DTIs networks compared with classic baselines. And then, its performance is further verified on a two-level DTIs signed network, and analyzed under different modes and settings. Finally, a case study is provided to verify our SHGNN-based DTI prediction.

1. Datasets

Two datasets are collected and their data statistics are shown in Table 3, where signed DTIs are labeled according to Table 1. Torres *et al.* [15] provided a signed DTIs network from early version of DrugBank. Here, we also extracted signed DTIs from a recent version of DrugBank [26], and additional information from related databases.

Dataset1 contains a signed bipartite network, which has 1178 drug nodes, 578 target nodes, and 2599 signed DTIs.

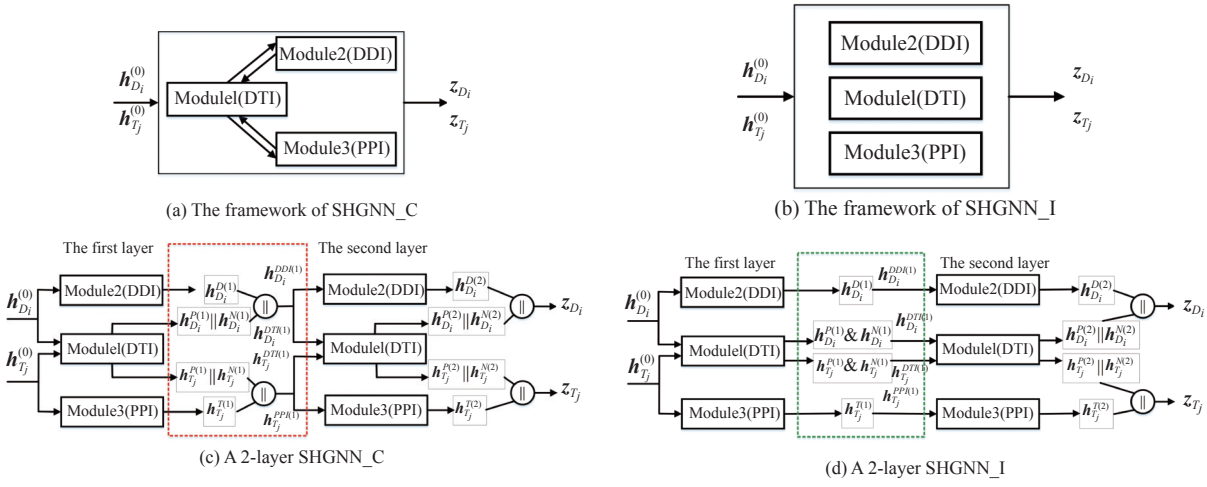

(a) The framework of SHGNN_C

(b) The framework of SHGNN_I

(c) A 2-layer SHGNN_C

(d) A 2-layer SHGNN_I

Figure 4 Two modes of SHGNNs and its 2-layer illustrative examples. (a) and (b) are the framework under cooperative mode and independent mode respectively. (c) and (d) are their 2-layer illustrative examples, in which the dashed boxes show their differences. "&" in (d) denotes "$\|$" or "$+$".

Table 3 Descriptions of datasets

	Drugs (features)	Target proteins	DTIs	DDIs	PPIs
Dataset1	1,178 (–)	578	+:1,093 −:1,506	–	–
Dataset2	846 (881)	685	+:909 −:1,859	169,162	5,820

Dataset2 contains a DTIs signed bipartite network, and additional DDIs and PPIs within these drugs and target proteins. It is processed as follows. According to statistics on DrugBank 5.1.7 [26], in commonly used drugs, the number of small molecule drugs can account for a high probability. And hence, we first collect approved small molecule drugs, and their target proteins. Also, we extract an unsigned DDIs network from DrugBank. Furthermore, we search the interaction information among target proteins from String 11.5 [33] database to build an unsigned PPIs network. The chemical structure information of the drug is additionally obtained from PubChem [32] database. Each drug is represented by a 881-dimensional binary vector, where 1 value indicates that the drug has a specific chemical structure segment. After discarding drugs not in PubChem [32] database and targets not in String 11.5 [33], we finally keep 846 drugs and 685 targets, 2768 signed DTIs, 169162 DDIs and 5820 PPIs.

2. Training settings and baselines

Settings of SHGNNs Here, we list SHGNN variants, hyper-parameters settings, and initial features of nodes.

- SHGNN variants. Given datasets with only DTIs networks, SHGNN in Algorithm 1 is employed. With additional DDIs and PPIs, SHGNNs in Algorithm 2 are trained under the cooperative mode or independent mode, as well as whether weight matrices are shared. Here, we use "_C" and "_I" to distinguish two training modes, and let "_S" denote sharing weights.
- Initial features of nodes. For convenience, we use "CS", "AD" and "AP" to represent cases of initial features. As summarized in Table 2, they correspond to chemical structures of drugs, the link vectors of drugs (i.e., one row in adjacency matrix $\boldsymbol{A}_D$), and the link vectors of targets (i.e., one row in adjacency matrix $\boldsymbol{A}_T$), respectively.
- Hyper-parameter settings. As shown in Table 4, SHGNNs employ $L=2$ convolutional layers and an Adam optimizer with a learning rate of 0.005. For simplicity, let drugs and targets have the same embedding dimensions d^{out} after all linear transformation, i.e., $\boldsymbol{h}_{D_i}^{P(l)}, \boldsymbol{h}_{D_i}^{N(l)}, \boldsymbol{h}_{D_i}^{D(l)}, \boldsymbol{h}_{T_j}^{P(l)}, \boldsymbol{h}_{T_j}^{N(l)}, \boldsymbol{h}_{T_j}^{T(l)} \in \mathbb{R}^{d^{\text{out}}}$. Here, we set $d^{\text{out}} \in \{8, 16, 32, 64, 128, 256\}$. We use different numbers of iterations to train the model and find that 2000 epochs are enough to achieve good results.

Table 4 Hyper-parameters of SHGNNs and GNNs baselines

Hyper-parameter	Value
Optimizer	Adam
Learning rate	0.005
Num of convolutional layers	2
Embedding dimension d_{out}	{8, 16, 32, 64, 128, 256}
Num of Epochs	2000

Baselines In this study, we take 5 models as baselines. The first kind is from traditional models. Here, we choose signed bipartite random walk (SBRW) [34]. With the help of the extended balanced theory, it carries out a random walk on signed bipartite networks. The second kind of baseline is from deep learning frameworks. We consider two most popular GNNs on unsigned graphs such as GCN [35] and GraphSAGE [36]. SBGNN [31] is a typical GNN model based on the extend balanced theory, and adapts to signed bipartite networks. We apply it to tackle with signed drug-target relations. The popular heterogeneous graph attention network (HAN) [37] is also tested on our datasets. It is a heterogeneous GNN model based on meta paths and hierarchical attention mechanisms.

- Code sources and configurations. Since SBRW and SBGNN are dedicated on signed bipartite networks, we run them only on DTIs subnetworks. Their official source codes are employed[*1][*2]. Since raw GCN and GraphSAGE adapt to unsigned networks, here we apply their PyG code versions[*3] into the underly unsigned graphs of signed DTIs networks and set the mean aggregator in GraphSAGE. When applying HAN to signed relations, we define different meta paths for positive and negative DTIs. Its DGL code version[*4] with 9-head attentions is employed here. For fair comparisons, all baselines are trained with the same loss function in this study.
- Hyper-parameter settings. All GNNs keep the same hyper-parameter settings as those of SHGNNs, as shown in Table 4. For SBRW, there are parameters including ω, δ_{p} and δ_n. ω is a bias parameter for random walkers. The thresholds δ_{p} and δ_n are used to define elements of adjacency matrices. Here, we varied $\omega \in \{1, 2, 3, 4, 5\}$, $\delta_{\text{p}} \in \{0, 25, 50, 75, 100\}$ and $\delta_n \in \{0, -25, -50, -75, -100\}$, and find that SBRW achieves optimal performance when $\omega = 2$, $\delta_{\text{p}} = 50$, $\delta_n = -100$.

3. Comparisons

We employ the area under the receiver operating characteristic curve (AUC), accuracy (ACC) and two F-score indicators to evaluate experimental results. A higher value of these metrics indicates better performance.

[*1] https://github.com/DSE-MSU/signed-bipartite-networks
[*2] https://github.com/huangjunjie-cs/SBGNN
[*3] https://github.com/pyg-team/pytorch_geometric
[*4] https://github.com/dmlc/dgl/tree/master/examples/pytorch/han

Each experiment run is 5-fold cross-validation (CV) and all the results are the statistical values across 5 runs. In CV experiments, we randomly divide all DTIs into 5 equal-size groups. 4-group DTIs serve as the training set and the rest one is used to test the model. All DDIs and (or) PPIs data are employed in training SHGNNs if the responding module is integrated. In Tables 5–7, we show the overview results of all methods in terms of best values over all settings. And Figure 5 shows detailed performance with different embedding dimensions. We report the average and the standard deviation (std) of these metrics across 5 runs.

Table 5 Comparisons of methods on the signed bipartite networks from dataset1 and dataset2

	Dataset1				Dataset2			
Methods	ACC	Macro-F1	Micro-F1	AUC	ACC	Macro-F1	Micro-F1	AUC
SBRW	$0.775_{\pm 0.013}$	$0.757_{\pm 0.012}$	$0.775_{\pm 0.013}$	$0.777_{\pm 0.015}$	$0.756_{\pm 0.018}$	$0.738_{\pm 0.018}$	$0.756_{\pm 0.018}$	$0.824_{\pm 0.012}$
SBGNN	$0.867_{\pm 0.006}$	$0.865_{\pm 0.006}$	$0.867_{\pm 0.006}$	$0.928_{\pm 0.017}$	$0.865_{\pm 0.015}$	$0.849_{\pm 0.015}$	$0.865_{\pm 0.015}$	$0.917_{\pm 0.019}$
GCN	$0.872_{\pm 0.002}$	$0.868_{\pm 0.008}$	$0.872_{\pm 0.002}$	$0.945_{\pm 0.003}$	$0.869_{\pm 0.012}$	$0.867_{\pm 0.013}$	$0.869_{\pm 0.012}$	$0.916_{\pm 0.006}$
GraphSAGE	$0.876_{\pm 0.008}$	$0.870_{\pm 0.008}$	$0.876_{\pm 0.008}$	$0.943_{\pm 0.003}$	$0.885_{\pm 0.007}$	$0.873_{\pm 0.007}$	$0.885_{\pm 0.007}$	$0.922_{\pm 0.004}$
HAN	$0.878_{\pm 0.004}$	$0.875_{\pm 0.003}$	$0.878_{\pm 0.004}$	$0.947_{\pm 0.003}$	$0.868_{\pm 0.003}$	$0.851_{\pm 0.003}$	$0.868_{\pm 0.003}$	$0.929_{\pm 0.002}$
SHGNN	$\mathbf{0.885}_{\pm 0.003}$	$\mathbf{0.882}_{\pm 0.003}$	$\mathbf{0.885}_{\pm 0.003}$	$\mathbf{0.950}_{\pm 0.006}$	$\mathbf{0.889}_{\pm 0.003}$	$\mathbf{0.874}_{\pm 0.006}$	$\mathbf{0.889}_{\pm 0.003}$	$\mathbf{0.935}_{\pm 0.004}$

Note: The highest score is in bold.

Table 6 Comparisons on the two-level signed heterogeneous network from the dataset2

Methods	ACC	Macro-F1	Micro-F1	AUC
GCN	$0.892_{\pm 0.003}$	$0.879_{\pm 0.003}$	$0.892_{\pm 0.003}$	$0.921_{\pm 0.007}$
GraphSAGE	$0.889_{\pm 0.003}$	$0.878_{\pm 0.002}$	$0.889_{\pm 0.003}$	$0.924_{\pm 0.002}$
HAN	$0.874_{\pm 0.003}$	$0.858_{\pm 0.003}$	$0.874_{\pm 0.003}$	$0.933_{\pm 0.004}$
SHGNN_I	$\underline{0.896}_{\pm 0.005}$	$\underline{0.884}_{\pm 0.010}$	$\underline{0.896}_{\pm 0.005}$	$\underline{0.935}_{\pm 0.010}$
SHGNN_C	$\mathbf{0.904}_{\pm 0.004}$	$\mathbf{0.889}_{\pm 0.006}$	$\mathbf{0.904}_{\pm 0.004}$	$\mathbf{0.938}_{\pm 0.006}$

Note: The best is marked in bold and the second best is in underline.

Table 7 The effect of different initial features of drug and target nodes on SHGNNs-based prediction methods

Methods	Feature	ACC	Macro-F1	Micro-F1	AUC
SHGNN_I (_S)	CS&AP	0.893 (0.893)	0.880 (0.877)	0.893 (0.893)	0.927 (0.928)
	CS‖AD&AP	0.892 (0.892)	0.884 (0.880)	0.892 (0.892)	0.933 (0.934)
	AD&AP	**0.896 (0.894)**	**0.884 (0.885)**	**0.896 (0.894)**	**0.935 (0.934)**
SHGNN_C (_S)	CS&AP	0.897 (0.891)	0.884 (0.879)	0.897 (0.891)	0.931 (0.930)
	CS‖AD&AP	0.899 (0.896)	0.887 (0.883)	0.899 (0.896)	0.935 (0.933)
	AD&AP	**0.904 (0.903)**	**0.889 (0.887)**	**0.904 (0.903)**	**0.938 (0.936)**

Note: The bold indicates the best within the group.
CS&AP: initial inputs include the chemical structures of drugs and the link vectors of targets.
AD&AP: initial inputs include link vectors of drugs and targets.
CS‖AD&AP: initial inputs include the concatenation of chemical structures and link vectors of drugs, and link vectors of targets.

The purpose of our experiments is to obtain the following observations: 1) the validity of the SHGNNs-DTI framework, not only on the signed bipartite network but also on the two-level heterogeneous network; 2) the effect of model settings and training modes on performance of SHGNNs.

From Table 5, we can find the performance of six methods on signed bipartite networks as shown in Figure 1 (a) from dataset1 and dataset2. Here, since attributes of drugs and targets are missing in dataset1, we employ the link vectors between drugs and targets as the initial features of nodes. Compared with SBRW and SBGNN, the performance of the SHGNN greatly exceeds those of the baseline methods. It hints that the extended balance theory, which is the underly basis of the two baselines, is not applicable between drugs and targets. Compared with GCN and GraphSAGE, SHGNN follows signs to aggregate messages from different kinds of neighbors, and hence it makes better use of signed graph structures. In addition, it is observed that, the meta-path based HAN, which also considers the link signs, is still inferior to our SHGNN model in all metrics values. In summary, SHGNN-DTI shows its significant better performance on predicting signed DTIs on bipartite networks.

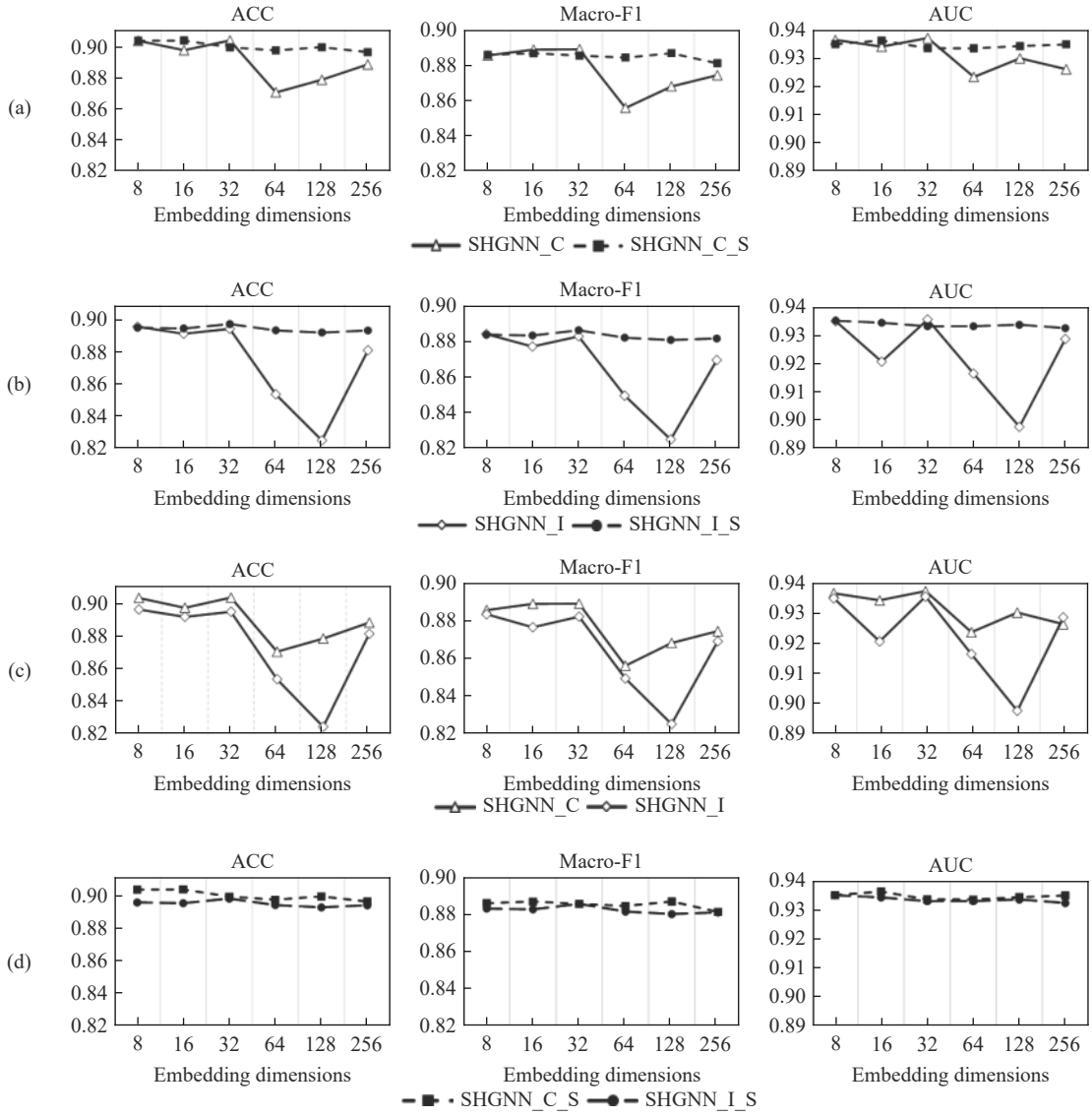

Figure 5 Comparison of three-module SHGNNs with different embedding dimensions on dataset2. (a) Comparison of SHGNN_C and its variant with sharing weights; (b) Comparison of SHGNN_I and its variant with sharing weights; (c) Comparison of SHGNN_C and SHGNN_I; (d) Comparison of SHGNN_C_S and SHGNN_I_S.

In Table 6, we can find the performance of SHGNNs and baselines on the two-level signed heterogeneous network (as shown in Figure 1(b)) from the dataset2. Firstly, both SHGNN_C and SHGNN_I are significantly superior to baselines such as GraphSAGE and HAN. Secondly, SHGNN_C performs better than SHGNN_I, and the observation will be further analyzed later. In addition, compared with the results of dataset2 shown in Table 5, SHGNNs and baselines promote almost all metric values. As a result, it illustrates benefits from DDIs and PPIs networks.

In Table 7, we show the effect of initial nodes features on SHGNN_C, SHGNN_I and their versions with sharing weights. Firstly, the model performance of SHGNN-DTI maintains a high level for all initial features. Secondly, it is observed that the best values of SHGNN generally occur in consideration of the link vector from $\boldsymbol{A}_D$ as the initial features of drugs, and the link vector from $\boldsymbol{A}_T$ as the initial features of targets. This may be caused by the inconsistency between the chemical structure features and the DTIs network.

In Figure 5, we further show the performance of SHGNN_C, SHGNN_I and their versions with sharing weights, in different embedding dimensions. Their Micro-F1 values are not illustrated, but they also have similar trends. Here, we employ the initial feature setting that can achieve the best performance (i.e. AD&AP). Firstly, versions with sharing weights are more stable, and their model performance maintains a high level for any embedding dimensions with the maximum difference between indicators not more than 1 percentage point. Secondly, SHGNN_C is better than SHGNN_I, which hints that when SHGNNs in cooperatively training mode, modules can interact with each other to capture the hidden information within signed heterogeneous networks.

Observations about the SHGNN-DTI can be con-

cluded as follows: 1) it is an effective way to predict signed DTIs; 2) DDIs and PPIs could provide benefits for promoting performance of SHGNNs; 3) the cooperative mode is better than the independent mode; 4) SHGNNs with sharing weights are more robust in terms of embedding dimensions.

4. Ablation study

In this section, we vary the configurations of SHGNNs to verify the role of modules. For the purpose of illustration, we conduct experiments on subnetworks extracted from dataset2. We consider several versions of SHGNNs as follows.

- SHGNN: the SHGNN model works on three modules.
- SHGNN (Wo_DDI): the SHGNN model works without the DDI network.
- SHGNN (Wo_PPI): the SHGNN model works without the PPI network.
- SHGNN (Wo_DTI): the SHGNN model works on DDIs and PPIs networks, i.e., without the DTI network.
- SHGNN (O_DTI): the SHGNN model works only on the signed bipartite DTI network, i.e., without DDIs and PPIs.

The last one runs Algorithm 1, while others run Algorithm 2 under the cooperative mode without sharing weights.

Figure 6 shows their best values of 5 runs of 5-fold CV experiments. Their Micro-F1 values are not illustrated, but they also have similar trends. When SHGNN works with all modules, it achieves the best performance, i.e., ACC: 0.904, Macro-F1: 0.889, Micro-F1: 0.904 and AUC: 0.938. Besides, we obtain some observations.

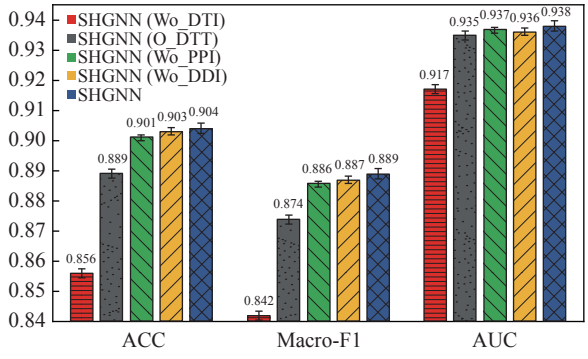

Figure 6 Ablation study results of the variants on dataset2.

i) Compared above results with those of SHGNN (Wo_DDI), SHGNN (Wo_PPI) and SHGNN (Wo_DTI), we find that missing any module will lead to performance degradation. When the DTI module is removed, scores of SHGNN decrease to ACC: 0.856, Macro-F1: 0.842, Micro-F1: 0.856 and AUC: 0.917. The largest gap between SHGNN (Wo_DTI) and SHGNN indicates that information within the DTI network is the most important in our model.

ii) The auxiliary role of DDI and PPI modules is illustrated. The performance of SHGNN (O_DTI), i.e., ACC 0.889, Macro-F1 0.874, Micro-F1 0.889 and AUC 0.935, is promoted when DDIs and (or) PPI networks are (is) integrated. It illustrates that they can provide additional information.

5. Case study

Here, we choose Goserelin and Epirubicin to verify our model's performance, as they are common and important drugs for the treatment of breast cancer that is the main cancer diagnosed in women. According to the announcement of the World Health Organization in December 2020, breast cancer has surpassed lung cancer as the most common cancer in the world [38], [39]. Goserelin is a synthetic analog of luteinizing hormone-releasing hormone, which can be used to treat breast cancer by reducing secretion of gonadotropins from the pituitary. Epirubicin is an anthracycline topoisomerase II inhibitor used as an adjuvant to treating axillary node metastases in patients who have undergone surgical resection of primary breast cancer.

However, we find in DrugBank [26] that the DTIs related to these two drugs are very few. Goserelin only contains two positive DTIs, and Epirubicin only contains two negative DTIs. Goserelin has "agonist" relations with Gonadotropin-releasing hormone receptor and Lutropin-choriogonadotropic hormone receptor. Meanwhile, Epirubicin has "antagonist" relation with Chromodomain-helicase-DNA-binding protein 1 (CHD1), and the "inhibitor" action mode on DNA topoisomerase 2-alpha. In this case study, we aim at verifying the validity of the model on discovering potential DTIs, via predicting all signed relations between both drugs and their interactions with all targets.

5 runs of 5-fold cross-validation experiments are conducted on SHGNN_C, to predict known DTIs for Goserelin and Epirubicin. The best model settings in above section is employed, i.e., without sharing weights, setting AD&AP for the initial features of nodes and the number of dimensions equal to 32. Table 8 shows DTIs within their top-10 ranks in terms of "softmax" values.

Top-10 DTIs of Goserelin Apoptosis regulator Bcl-2 is the predicted target protein with the largest score in the DTIs predicted to be positive. As reported in the literature [40], Goserelin results in increased expression of Bcl-2 protein. Goserelin is shown in DrugBank [26] as an agonist of Gonadotropin-releasing hormone receptor and Lutropin-choriogonadotropic hormone receptor. Two target proteins of DTIs predicted to be negative, Plasma kallikrein and Transmembrane protein serine 2, have also been confirmed by literature [41]. Among the DTIs with the top-10 prediction scores, no relevant evidence was found for the DTIs between Goserelin and Synaptic vesicle glycoprotein 2A, Androgen receptor, Somatostatin receptor, Sterol o-acyltransferase 1 and Osteocalcin, leaving for further study.

Top-10 DTIs of Epirubicin The probably positive

Table 8 Top-10 DTIs predicted by SHGNN for Goserelin and Epirubicin

Drug	Target	Sign	Evidence
Goserelin	Apoptosis regulator Bcl-2	+	Goserelin results in increased expression of Bcl-2 protein [40]
	Synaptic vesicle glycoprotein 2A	+	Null
	Androgen receptor	−	Null
	Gonadotropin-releasing hormone receptor	+	Agonist in DrugBank
	Lutropin-choriogonadotropic hormone receptor	+	Agonist in DrugBank
	Plasma kallikrein	−	Goserelin inhibited cell growth and Plasma kallikrein protein secretion in LNCaP and C4-2 cells [41]
	Somatostatin receptor	+	Null
	Transmembrane protein serine 2	−	When treated with the combination of Goserelin and Bicalutamide, Transmembrane protein serine 2 was strongly inhibited in benign glands and moderately inhibited in malignant glands [41]
	Sterol o-acyltransferase 1	−	Null
	Osteocalcin	−	Null
Epirubicin	Caspase-3	+	Epirubicin results in increased activity of Caspase-3 protein [42]
	ATP-binding cassette sub-family G member 1	+	Epirubicin analog results in increased expression of ATP-binding cassette sub-family G member 1 mRNA [43]
	Fatty acid-binding protein	+	Null
	Estrogen receptor alpha	−	Epirubicin binds to and results in decreased activity of Estrogen receptor alpha protein [44]
	Serine/threonine-protein kinase mTOR	+	Null
	Estrogen receptor beta	−	Epirubicin binds to and results in decreased activity of Estrogen receptor beta protein [44]
	Nucleolar and coiled-body phosphoprotein 1	−	Null
	Synaptic vesicle glycoprotein 2A	−	Null
	DNA topoisomerase 2-alpha	−	Inhibitor in DrugBank
	Estrogen sulfotransferase	−	Null

DTI related to Caspase-3 is supported in literature [42], where Epirubicin was demonstrated to result in increased activity of Caspase-3 protein. The link sign between Epirubicin and ATP-binding cassette sub-family G member 1 is also predicted to be positive, which agrees with that Epirubicin analog results in increased expression of ATP-binding cassette sub-family G member 1 mRNA [43]. Within the negative DTIs, Epirubicin is predicted to interact with Estrogen receptor alpha (ERα) and Estrogen receptor beta (ERβ). Estrogen antagonists and drugs that reduce estrogen biosynthesis have become highly successful therapeutic agents for breast cancer patients, the effects of estrogen are largely mediated by ERα and ERβ [45]. A previous study [44] has shown that Epirubicin binds to and results in decreased activity of ERα and ERβ. DNA topoisomerase 2-alpha as an inhibitor in DrugBank [26], is predicted to be negatively related to Epirubicin. However, unconfirmed DTIs are still present in the predicted results of Epirubicin, including Fatty acid-binding protein, Serine/threonine-protein kinase mTOR, Nucleolar and coiled-body phosphoprotein 1, Synaptic vesicle glycoprotein 2A, and Estrogen sulfotransferase.

In addition, Synaptic vesicle glycoprotein 2A is present in the top 10 DTIs for both Goserelin and Epirubicin, which are unproven DTIs in the relevant databases or literatures. In descriptions of DrugBank [26], Levetiracetam acts as an agonist of Synaptic vesicle glycoprotein 2A to treat various types of seizures caused by epilepsy. This means that Goserelin and Epirubicin may also be used as adjuvant treatment for such diseases.

In summary, half of 20 signed DTIs have evidence in DrugBank [26] or have support in related literature. Although the known record between Epirubicin and CHD1 is not included within the Top-10 ranks, its score is still very high and it belongs to top-50 DTIs of Epirubicin. Especially, 7 records are out of DrugBank [26], which further verifies the model performance in predicting new signed DTIs.

V. Conclusions

DTIs prediction is a potential way to discover the types of relations between drugs and target proteins, which is of great significance for pharmaceutical medicine. Existing computational methods can screen potential DTIs from a large number of drug pairs at low cost, but they are mostly unable to predict specific types of DTIs, such as positive and negative DTIs. In this paper, the DTIs prediction problem is regarded as the sign prediction problem on signed heterogeneous networks,

and an end-to-end prediction method based on the signed heterogeneous graph neural networks (SHGNNs) is proposed to predict the link signs between drugs and targets. When designing SHGNNs, we dedicate message passing and aggregation on signed bipartite networks, and additionally incorporate DDIs and PPIs information, further try several training modes. The performance of the SHGNNs-based prediction method greatly exceeds those of the baseline methods. We test the method with different settings, including its working modes, embedding dimensions and initial features. In the case study, two drugs for breast cancer are chosen for DTIs prediction and the results show feasibility of our method.

In future research, we will extend our method to cold-start DTIs prediction problems with unknown drugs and targets and consider multi-modal node attributes to further improve the prediction performance.

Acknowledgement

This work was supported by the Shenzhen Science and Technology Program (Grant No. KQTD20200820113106007), the National Natural Science Foundation of China (Grant No. U22A2041, 61972451, and 62272288), the Guangdong Provincial Key Laboratory of Interdisciplinary Research and Application for Data Science, BNU-HKBU United International College (Grant No. 2022B1212010006), the Scientific Research Fund of Hunan Provincial Education Department of China (Grant No. 22B0097), and the Changsha Natural Science Foundation of China (Grant No. kq2202248).

References

[1] X. Q. Ru, X. C. Ye, T. Sakurai, *et al.*, "Current status and future prospects of drug-target interaction prediction," *Briefings in Functional Genomics*, vol. 20, no. 5, pp. 312–322, 2021.

[2] X. Chen, C. C. Yan, X. T. Zhang, *et al.*, "Drug-target interaction prediction: Databases, web servers and computational models," *Briefings in Bioinformatics*, vol. 17, no. 4, pp. 696–712, 2016.

[3] C. C. Wang, Y. Zhao, and X. Chen, "Drug-pathway association prediction: From experimental results to computational models," *Briefings in Bioinformatics*, vol. 22, no. 3, article no. bbaa061, 2021.

[4] W. Zhang, W. R. Lin, D. Zhang, *et al.*, "Recent advances in the machine learning-based drug-target interaction prediction," *Current Drug Metabolism*, vol. 20, no. 3, pp. 194–202, 2019.

[5] Y. Pan, X. J. Lei, and Y. C. Zhang, "Association predictions of genomics, proteinomics, transcriptomics, microbiome, metabolomics, pathomics, radiomics, drug, symptoms, environment factor, and disease networks: A comprehensive approach," *Medicinal Research Reviews*, vol. 42, no. 1, pp. 441–461, 2022.

[6] X. H. Wu, J. W. Duan, Y. Pan, *et al.*, "Medical knowledge graph: Data sources, construction, reasoning, and applications," *Big Data Mining and Analytics*, vol. 6, no. 2, pp. 201–217, 2023.

[7] R. Li, X. Yuan, M. Radfar, *et al.*, "Graph signal processing, graph neural network and graph learning on biological data: A systematic review," *IEEE Reviews in Biomedical Engineering*, vol. 16, pp. 109–135, 2023.

[8] X. Chen, N. N. Guan, Y. Z. Sun, *et al.*, "MicroRNA-small molecule association identification: From experimental results to computational models," *Briefings in Bioinformatics*, vol. 21, no. 1, pp. 47–61, 2020.

[9] G. Z. Zhang, M. L. Li, H. Deng, *et al.*, "SGNNMD: Signed graph neural network for predicting deregulation types of miRNA-disease associations," *Briefings in Bioinformatics*, vol. 23, no. 1, article no. bbab464, 2022.

[10] L. Guo, X. J. Lei, M. Chen, *et al.*, "MSResG: Using GAE and residual GCN to predict drug–drug interactions based on multi-source drug features," *Interdisciplinary Sciences: Computational Life Sciences*, vol. 15, no. 2, pp. 171–188, 2023.

[11] Y. C. Zhang, X. J. Lei, Y. Pan, *et al.*, "Drug repositioning with GraphSAGE and clustering constraints based on drug and disease networks," *Frontiers in Pharmacology*, vol. 13, article no. 872785, 2022.

[12] G. Zhao, Q. G. Wang, F. Yao, *et al.*, "Survey on large-scale graph neural network systems," *Journal of Software*, vol. 33, no. 1, pp. 150–170, 2022. (in Chinese)

[13] L. Zhang, C. C. Wang, and X. Chen, "Predicting drug-target binding affinity through molecule representation block based on multi-head attention and skip connection," *Briefings in Bioinformatics*, vol. 23, no. 6, article no. bbac468, 2022.

[14] H. Z. Wang, F. Huang, Z. K. Xiong, *et al.*, "A heterogeneous network-based method with attentive meta-path extraction for predicting drug-target interactions," *Briefings in Bioinformatics*, vol. 23, no. 4, article no. bbac184, 2022.

[15] N. B. Torres and C. Altafini, "Drug combinatorics and side effect estimation on the signed human drug-target network," *BMC Systems Biology*, vol. 10, no. 1, article no. 74, 2016.

[16] B. F. Hu, H. Wang, and Z. M. Yu, "Drug side-effect prediction via random walk on the signed heterogeneous drug network," *Molecules*, vol. 24, no. 20, article no. 3668, 2019.

[17] Y. F. Shang, L. Gao, Q. Zou, *et al.*, "Prediction of drug-target interactions based on multi-layer network representation learning," *Neurocomputing*, vol. 434, pp. 80–89, 2021.

[18] Y. X. Gong, B. Liao, P. Wang, *et al.*, "DrugHybrid_BS: Using hybrid feature combined with bagging-SVM to predict potentially druggable proteins," *Frontiers in Pharmacology*, vol. 12, article no. 771808, 2021.

[19] Y. Y. Chu, A. C. Kaushik, X. G. Wang, *et al.*, "DTI-CDF: A cascade deep forest model towards the prediction of drug-target interactions based on hybrid features," *Briefings in Bioinformatics*, vol. 22, no. 1, pp. 451–462, 2021.

[20] Y. J. Ding, J. J. Tang, F. Guo, *et al.*, "Identification of drug-target interactions via multiple kernel-based triple collaborative matrix factorization," *Briefings in Bioinformatics*, vol. 23, no. 2, article no. bbab582, 2022.

[21] X. Chen, M. X. Liu, and G. Y. Yan, "Drug-target interaction prediction by random walk on the heterogeneous network," *Molecular BioSystems*, vol. 8, no. 7, pp. 1970–1978, 2012.

[22] Y. C. Zhang, X. J. Lei, Z. Q. Fang, *et al.*, "CircRNA-disease associations prediction based on metapath2vec++ and matrix factorization," *Big Data Mining and Analytics*, vol. 3, no. 4, pp. 280–291, 2020.

[23] X. Liu and M. Yang, "Research on conversational machine reading comprehension based on dynamic graph neural network," *Journal of Integration Technology*, vol. 11, no. 2, pp. 67–78, 2022. (in Chinese)

[24] Y. Y. Wang, X. J. Lei, Y. Pan, "Predicting microbe-disease association based on heterogeneous network and global graph feature learning," *Chinese Journal of Electronics*, vol. 31, no. 2, pp. 345–353, 2022.

[25] H. T. Fu, F. Huang, X. Liu, *et al.*, "MVGCN: Data integration through multi-view graph convolutional network for predicting links in biomedical bipartite networks," *Bioinformatics*, vol. 38, no. 2, pp. 426–434, 2022.

[26] D. S. Wishart, Y. D. Feunang, A. C. Guo, *et al.*, "DrugBank 5.0: A major update to the drugbank database for 2018," *Nucleic Acids Research*, vol. 46, no. D1, pp. D1074–D1082, 2018.

[27] T. Lee and Y. Yoon, "Drug repositioning using drug-disease vectors based on an integrated network," *BMC Bioinformatics*, vol. 19, no. 1, article no. 446, 2018.

[28] M. Chen, Y. Pan, and C. Y. Ji, "Predicting drug drug interactions by signed graph filtering-based convolutional networks," in *Proceedings of the 17th International Symposium on Bioinformatics Research and Applications*, Shenzhen, China, pp. 375–387, 2021.
[29] M. Chen, W. Jiang, Y. Pan, *et al.*, "SGFNNs: Signed graph filtering-based neural networks for predicting drug–drug interactions," *Journal of Computational Biology*, vol. 29, no. 10, pp. 1104–1116, 2022.
[30] T. Derr, Y. Ma, and J. L. Tang, "Signed graph convolutional networks," in *Proceedings of 2018 IEEE International Conference on Data Mining*, Singapore, pp. 929–934, 2018.
[31] J. J. Huang, H. W. Shen, Q. Cao, *et al.*, "Signed bipartite graph neural networks," in *Proceedings of the 30th ACM International Conference on Information & Knowledge Management*, Queensland, Australia, pp. 740–749, 2021.
[32] S. Kim, J. Chen, T. J. Cheng, *et al.*, "PubChem in 2021: New data content and improved web interfaces," *Nucleic Acids Research*, vol. 49, no. D1, pp. D1388–D1395, 2021.
[33] D. Szklarczyk, A. L. Gable, K. C. Nastou, *et al.*, "The string database in 2021: Customizable protein–protein networks, and functional characterization of user-uploaded gene/measurement sets," *Nucleic Acids Research*, vol. 49, no. D1, pp. D605–D612, 2021.
[34] T. Derr, C. Johnson, Y. Chang, *et al.*, "Balance in signed bipartite networks," in *Proceedings of the 28th ACM International Conference on Information and Knowledge Management*, Beijing, China, pp. 1221–1230, 2019.
[35] T. N. Kipf and M. Welling, "Semi-supervised classification with graph convolutional networks," in *Proceedings of the 5th International Conference on Learning Representations*, Toulon, France, 2017.
[36] W. L. Hamilton, R. Ying, and J. Leskovec, "Inductive representation learning on large graphs," in *Proceedings of the 31st International Conference on Neural Information Processing Systems*, Long Beach, CA, USA, pp. 1025–1035, 2017.
[37] X. Wang, H. Y. Ji, C. Shi, *et al.*, "Heterogeneous graph attention network," in *Proceedings of the World Wide Web Conference*, San Francisco, CA, USA, pp. 2022–2032, 2019.
[38] A. T. Jacobs, D. M. Castaneda-Cruz, M. M. Rose, *et al.*, "Targeted therapy for breast cancer: An overview of drug classes and outcomes," *Biochemical Pharmacology*, vol. 204, article no. 115209, 2022.
[39] Y. S. Lu, K. S. Lee, T. Y. Chao, *et al.*, "A phase IB study of alpelisib or buparlisib combined with tamoxifen plus goserelin in premenopausal women with HR-positive HER2-negative advanced breast cancer," *Clinical Cancer Research*, vol. 27, no. 2, pp. 408–417, 2021.
[40] Y. B. Baytur, K. Ozbilgin, S. Cilaker, *et al.*, "A comparative study of the effect of raloxifene and gosereline on uterine leiomyoma volume changes and estrogen receptor, progesterone receptor, bcl-2 and p53 expression immunohistochemically in premenopausal women," *European Journal of Obstetrics & Gynecology and Reproductive Biology*, vol. 135, no. 1, pp. 94–103, 2007.
[41] E. A. Mostaghel, P. S. Nelson, P. Lange, *et al.*, "Targeted androgen pathway suppression in localized prostate cancer: A pilot study," *Journal of Clinical Oncology*, vol. 32, no. 3, pp. 229–237, 2014.
[42] Y. L. Lo and W. Wang, "Formononetin potentiates epirubicin-induced apoptosis via ROS production in HeLa cells *in vitro*," *Chemico-Biological Interactions*, vol. 205, no. 3, pp. 188–197, 2013.
[43] Y. L. Lo and W. C. Tu, "Co-encapsulation of chrysophsin-1 and epirubicin in PEGylated liposomes circumvents multidrug resistance in HeLa cells," *Chemico-Biological Interactions*, vol. 242, pp. 13–23, 2015.
[44] F. Fan, R. Hu, A. Munzli, *et al.*, "Utilization of human nuclear receptors as an early counter screen for off-target activity: A case study with a compendium of 615 known drugs," *Toxicological Sciences*, vol. 145, no. 2, pp. 283–295, 2015.
[45] H. Hua, H. Y. Zhang, Q. B. Kong, *et al.*, "Mechanisms for estrogen receptor expression in human cancer," *Experimental Hematology & Oncology*, vol. 7, article no. 24, 2018.

Ming CHEN is currently a Lecturer in the College of Information Science and Engineering at Hunan Normal University, Changsha, China. She received the M.S. degree in 2007 from Hunan Normal University, and the Ph.D. degree in 2012 from Wuhan University. Her current research interests mainly include graph signal processing and deep learning. (Email: chenming@hunnu.edu.cn)

Yajian JIANG is currently an M.S. student in the College of Information Science and Engineering, Hunan Normal University. His current research interests include bioinformatics, data mining, and deep learning.
(Email: j__yj2020@hunnu.edu.cn)

Xiujuan LEI is currently a Professor in the School of Computer Science at Shaanxi Normal University, Xi'an, China. She received the M.S. and Ph.D. degrees from Northwestern Polytechnical University, Xi'an, China, in 2001 and 2005, respectively. Her current research interests mainly include intelligent computing and bioinformatics. (Email: xjlei@snnu.edu.cn)

Yi PAN is currently a Professor of the Faculty of Computer Science and Control Engineering, Shenzhen Institute of Advanced Technology, Chinese Academy of Sciences. He received the B.E. and M.E. degrees in computer engineering from Tsinghua University, China, in 1982 and 1984, respectively, and the Ph.D. degree in computer science from the University of Pittsburgh, USA, in 1991. His current research interests include bioinformatics and health informatics using big data analytics, cloud computing, and machine learning technologies. (Email: yi.pan@siat.ac.cn)

Chunyan JI is currently an Assistant Professor in Department of Computer Science of BNU-HKBU United International College. She received the M.S. and Ph.D. degrees in computer science from Georgia State University. Her main research areas include deep learning, bioinformatics and sound event detection. (Email: chunyanji@uic.edu.cn)

Wei JIANG is currently an M.S. student in the College of Information Science and Engineering, Hunan Normal University. His current research interests include graph signal processing and deep learning.
(Email: jw2020@smail.hunnu.edu.cn)